

High Performance Parallel Algorithms for the Tucker Decomposition of Sparse Tensors

Oguz Kaya
INRIA and LIP, ENS Lyon
Lyon, France
oguz.kaya@ens-lyon.fr

Bora Uçar
CNRS and LIP, ENS Lyon
Lyon, France
bora.ucar@ens-lyon.fr

Abstract—We investigate an efficient parallelization of a class of algorithms for the well-known Tucker decomposition of general N -dimensional sparse tensors. The targeted algorithms are iterative and use the alternating least squares method. At each iteration, for each dimension of an N -dimensional input tensor, the following operations are performed: (i) the tensor is multiplied with $(N - 1)$ matrices (TTMc step); (ii) the product is then converted to a matrix; and (iii) a few leading left singular vectors of the resulting matrix are computed (TRSVD step) to update one of the matrices for the next TTMc step. We propose an efficient parallelization of these algorithms for the current parallel platforms with multicore nodes. We discuss a set of preprocessing steps which takes all computational decisions out of the main iteration of the algorithm and provides an intuitive shared-memory parallelism for the TTM and TRSVD steps. We propose a coarse and a fine-grain parallel algorithm in a distributed memory environment, investigate data dependencies, and identify efficient communication schemes. We demonstrate how the computation of singular vectors in the TRSVD step can be carried out efficiently following the TTMc step. Finally, we develop a hybrid MPI-OpenMP implementation of the overall algorithm and report scalability results on up to 4096 cores on 256 nodes of an IBM BlueGene/Q supercomputer.

Keywords-sparse tensors, parallel tensor factorization, Tucker decomposition, higher order orthogonal iteration

I. INTRODUCTION

Tensors or multi-dimensional arrays are used to represent data with high dimensionality in many applications. Among the most popular of these applications are the analysis of Web graphs [1], forming knowledge bases [2], [3], item and tag recommendations [4], [5], [6], chemometrics [7], signal processing [8], computer vision [9], and forensic data analysis [10]. In these applications, tensor decomposition algorithms are used to find latent relations or predict missing elements in the data using its low rank structure. There are two prominent tensor decomposition formulations. *CANDECOMP/PARAFAC* (CP) decomposition formulates a tensor as a sum of rank-one tensors. *Tucker* formulation expresses a tensor with a smaller core tensor multiplied by a matrix along each dimension—see Fig. 1 for a simplistic view. Both of these formulations have uses in various applications; in particular, the CP formulation is deemed useful for understanding latent components, whereas the Tucker formulation is considered to be more appropriate for compression [11], identifying relations among the factors [12], and predicting missing data entries [4]. Tucker

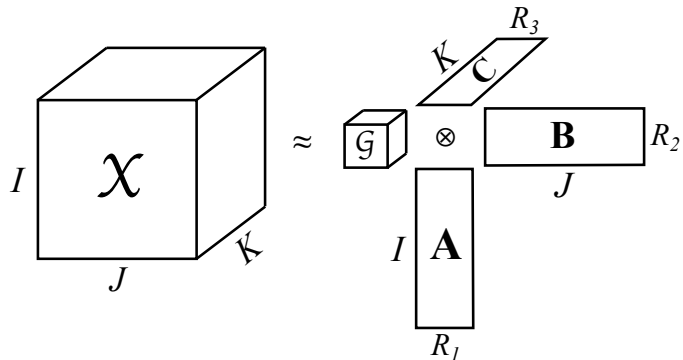


Fig. 1: Tucker decomposition of a 3rd mode tensor $\mathcal{X} \in \mathbb{R}^{I_1 \times I_2 \times I_3}$ as a core tensor $\mathcal{G} \in \mathbb{R}^{R_1 \times R_2 \times R_3}$ multiplied by matrices $\mathbf{A} \in \mathbb{R}^{I_1 \times R_1}$, $\mathbf{B} \in \mathbb{R}^{I_2 \times R_2}$ and $\mathbf{C} \in \mathbb{R}^{I_3 \times R_3}$ in different modes. In the CP-decomposition, \mathcal{G} is a diagonal tensor having the same size along each dimension, and \mathbf{A} , \mathbf{B} and \mathbf{C} have the same number of columns.

decomposition and its variants are known to be more effective tools for data analysis at the expense of higher computational requirements, and many of its variants have been employed in data analysis problems [4], [5], [6]. In these applications, the tensor formed from the data is sparse, which can adequately be exploited to compute the Tucker decomposition more efficiently. With this motivation, we investigate the efficient parallel computation of the low rank Tucker decomposition of sparse tensors in shared and distributed memory environments.

There are variants of CP and Tucker decompositions, and different algorithms to compute them [13], [14]. The most common algorithms for both decompositions and their variants are based on the alternating least squares (ALS) method. The algorithms of this type are iterative, where the computational core of an iteration is a special operation performed on an N -mode tensor and N matrices. The key operation in the ALS-based CP decomposition (CP-ALS) case is called the matrix-cized tensor times Khatri-Rao product; we refer the reader to other resources for details [14]. The key operation in the ALS-based Tucker decomposition algorithm, namely Higher Order Orthogonal Iteration (HOOI) [15], is called *tensor times matrix-chain* product. These two operations pose similar computational challenges; but there are distinct opportunities for parallel efficiency.

The tensor times matrix-chain (TTMc) product in the HOOI

algorithm is performed for all modes of the N -mode input tensor in sequence, at every ALS iteration. TTMc for a mode n involves tensor times matrix (TTM) products with $N - 1$ different matrices, each of which is associated with one of the modes other than n . TTM product can be considered as a higher dimensional variant of the matrix-vector multiply operation (Section II explains the TTM operation in detail). Techniques for efficiency of a single TTM are therefore akin to those used in the matrix-vector multiplication but require more effort to overcome the difficulties associated with the higher dimensionality.

Following the TTMc step for each mode, HOOI algorithm computes a few singular vectors of a large, usually tall-and-skinny dense matrix at every ALS iteration. This matrix arises from a logical reorganization of the result of the TTMc associated with the corresponding mode. The cost of computing the singular vectors is not negligible and hence needs to be addressed in an efficient parallelization of the HOOI algorithm. We refer to the computation of the desired singular vectors as the truncated SVD (TRSVD) step.

Our contributions are as follows. First, we design efficient parallel algorithms for the TTMc operation on sparse tensors. To this end, we first introduce a particular nonzero-based reformulation of TTMc. Using this formulation, we then introduce a preprocessing step called symbolic TTMc to identify data dependencies and perform all index computations before the HOOI iterations for efficiency. Then, we provide a shared-memory parallel algorithm for the main iteration of HOOI which makes use of the symbolic TTMc step. Second, we introduce a coarse and a fine-grain task definition for TTMc and TRSVD steps within the HOOI algorithm, and propose a hybrid shared-distributed memory parallel algorithm based on the distribution of these tasks. We discuss the computational and communication requirements of the algorithm for a given task distribution, and make use of the hypergraph models from our earlier work on CP-ALS [16] for reducing communication and achieving load balance during each HOOI iteration. Third, we stress how to efficiently perform the TRSVD step in a distributed memory setting, and make use of the PETSc [17] and SLEPc [18] libraries in this step. We carefully designed this step so that the communication requirements in parallel iterative algorithms used for computing the singular vectors are reduced, and the load balance is achieved by making use of the data decomposition of the TTMc step. Finally, we propose an efficient OpenMP-MPI hybrid parallel implementation of the HOOI algorithm in C++, and present scalability results on a high-end parallel system using up to 4096 cores on real world tensors. To the best of our knowledge, this is the first high performance parallel implementation of the HOOI algorithm for sparse tensors in shared/distributed memory environments using OpenMP/MPI.

The organization is as follows. We give background on the basic tensor operations, and a reformulation of the TTMc operation for sparse tensors in the next section. Then, in Section III, we propose shared and distributed memory parallel HOOI algorithms and discuss in detail the TTMc and the

TRSVD steps. Next, we give a brief summary of related recent work in Section IV. Finally, we provide experimental results in Section V, and conclude the paper in Section VI.

II. BACKGROUND

We use bold, upper case Roman letters for matrices, as in \mathbf{A} . Matrix elements are shown with the corresponding lowercase letters, as in $a_{i,j}$. Matlab notation is used to refer to the entire rows and columns of a matrix, e.g., $\mathbf{A}(i, :)$ and $\mathbf{A}(:, j)$ refer to the i th row and j th column of \mathbf{A} , respectively.

We use calligraphic fonts to refer to tensors, e.g., \mathcal{X} . The *order* of a tensor is the number of its dimensions or modes, which we denote with N . For the sake of simplicity of the notation and the discussion, we sometimes discuss the case $N = 3$, even though our algorithms and implementations have no such restriction. We explicitly generalize the discussion to order- N tensors whenever necessary. As in matrices, an element of a tensor is denoted by a lowercase letter and subscripts corresponding to the indices of the element, e.g., the element (i, j, k) of \mathcal{X} is $x_{i,j,k}$. A *fiber* of a tensor is defined by fixing every index but one, and a *slice* of a tensor is obtained by fixing only one index. For instance, for a third order tensor \mathcal{X} , $\mathcal{X}_{:,j,k}$ and $\mathcal{X}_{i,:}$ are fibers and $\mathcal{X}_{i,:,:}$ and $\mathcal{X}_{:,:k}$ are slices in the first and the third modes, respectively.

The *Kronecker product* of two vectors $u \in \mathbb{R}^I$ and $v \in \mathbb{R}^J$ results in a vector $w = u \otimes v$ where $w \in \mathbb{R}^{IJ}$ and $w_{j+(i-1)J} = u_i v_j$. We denote the *outer product* of the same vectors u and v as $\mathbf{W} = u \circ v$, where $\mathbf{W} \in \mathbb{R}^{I \times J}$ and $w_{i,j} = u_i v_j$. In general, performing the outer product of N vectors produces an N -dimensional tensor.

We reproduce the following definitions from Kolda and Bader's survey [14]. The n -mode *matricization* of a tensor \mathcal{X} is denoted by $\mathbf{X}_{(n)}$ and refers to the reordering of \mathcal{X} 's elements into a matrix by arranging the mode- n fibers as the columns of $\mathbf{X}_{(n)}$. For example, for $\mathcal{X} \in \mathbb{R}^{I_1 \times \dots \times I_N}$, $\mathbf{X}_{(1)} \in \mathbb{R}^{I_1 \times (I_2 \dots I_N)}$ denotes the mode-1 matricization of \mathcal{X} , where the rows of $\mathbf{X}_{(1)}$ correspond to the first mode of \mathcal{X} , and the columns correspond to the remaining modes. The tensor element x_{i_1, \dots, i_N} corresponds to the element $\left(i_1, 1 + \sum_{j=2}^N \left[(i_j - 1) \prod_{k=1}^{j-1} I_k \right] \right)$ of $\mathbf{X}_{(1)}$.

The n -mode *product* of a tensor $\mathcal{X} \in \mathbb{R}^{I_1 \times \dots \times I_N}$ with a matrix $\mathbf{U} \in \mathbb{R}^{J \times I_n}$ is denoted by $\mathcal{X} \times_n \mathbf{U}$. This is also referred to as tensor times matrix (TTM) product. The result \mathcal{Y} is a tensor of size $I_1 \times \dots \times I_{n-1} \times J \times I_{n+1} \times \dots \times I_N$. A particular element of \mathcal{Y} is given by

$$y_{i_1, \dots, i_{n-1}, j, i_{n+1}, \dots, i_N} = \sum_{i_n=1}^{I_n} x_{i_1, i_2, \dots, i_N} u_{j i_n} \quad (1)$$

A tensor can be multiplied by a set of matrices along a given set S of modes. We use the notation $\text{TTMc}(\mathcal{X}, S, \{\mathbf{U}_n : \text{for } n \in S\})$ to refer to the tensor n -mode product of \mathcal{X} with matrices \mathbf{U}_n for $n \in S$. We use $\text{TTMc}(S)$ for clarity, as the tensor \mathcal{X} and the matrices \mathbf{U}_n 's will be clear from the context. The operation $\mathcal{Y} \leftarrow \mathcal{X} \times_1 \mathbf{U}_1 \cdots \times_{n-1} \mathbf{U}_{n-1} \times_{n+1} \mathbf{U}_{n+1} \cdots \times_N \mathbf{U}_N$ stands for the TTMc of a tensor in all modes

except n , which we denote as $\mathcal{X} \times_{-n} \mathbf{U}_n$, or equivalently, $\text{TTMc}(\{1 \dots N\} \setminus \{n\})$.

The Tucker decomposition expresses a given tensor $\mathcal{X} \in \mathbb{R}^{I_1 \times \dots \times I_N}$ as a core tensor \mathcal{G} multiplied by a factor matrix \mathbf{U}_n of size $I_n \times R_n$ in each mode n . Here, R_1, \dots, R_N are the requested rank of the decomposition for each mode. Formally, the Tucker decomposition $[\mathcal{G}; \mathbf{U}_1, \dots, \mathbf{U}_N]$ writes \mathcal{X} as $\mathcal{G} \times_1 \mathbf{U}_1 \times_2 \dots \times_N \mathbf{U}_N$. For example, if $\mathcal{X} \in \mathbb{R}^{I_1 \times I_2 \times I_3}$, then in its Tucker decomposition $[\mathcal{G}; \mathbf{A}, \mathbf{B}, \mathbf{C}]$ we have $x_{i,j,k} \approx \sum_{p=1}^{I_1} \sum_{q=1}^{I_2} \sum_{r=1}^{I_3} g_{pqr} a_{ip} b_{jq} c_{kr}$.

A well-known algorithm for computing the Tucker decomposition is called the higher order orthogonal iteration (HOOI) [19], and is given in Algorithm 1. In this algorithm, the factor matrices are initialized first. This initialization could be done randomly or using the higher-order SVD [19]. Then, the ‘‘repeat-until’’ loop applies the alternating least squares method. Here, for each mode n , $\text{TTMc}(\{1, \dots, N\} \setminus \{n\})$ at Line 4 is computed. This produces a tensor of size $R_1 \times R_2 \times \dots \times R_{n-1} \times I_n \times R_{n+1} \times \dots \times R_N$, which is then matricized along the n th mode into the matrix $\mathbf{Y}_{(n)} \in \mathbb{R}^{I_n \times \prod_{i \neq n} R_i}$. Then, the leading R_n left singular vectors of $\mathbf{Y}_{(n)}$ are computed and used as the columns of \mathbf{U}_n at Line 5. After all matrices \mathbf{U}_n are updated, the core tensor \mathcal{G} is formed at Line 6, and the change in the fit measure $(|\mathcal{X}| - |\mathcal{G}|)/|\mathcal{X}|$ is checked at the end of each iteration.

Algorithm 1 HOOI algorithm for N -mode tensors

Input: \mathcal{X} : An N -mode tensor

R_1, \dots, R_N :

The rank of the decomposition for each mode

Output: Tucker decomposition $[\mathcal{G}; \mathbf{U}_1, \dots, \mathbf{U}_N]$

- 1: Initialize the matrix $\mathbf{U}_n \in \mathbb{R}^{I_n \times R_n}$ for $n = 1, \dots, N$
 - 2: **repeat**
 - 3: **for** $n = 1, \dots, N$ **do**
 - 4: $\mathcal{Y} \leftarrow \mathcal{X} \times_{-n} \mathbf{U}_n^T$
 - 5: $\mathbf{U}_n \leftarrow R_n$ leading left singular vectors of $\mathbf{Y}_{(n)}$
 - 6: $\mathcal{G} \leftarrow \mathcal{X} \times_1 \mathbf{U}_1^T \times_2 \dots \times_N \mathbf{U}_N^T$
 - 7: **until** no improvement or maximum iterations reached
 - 8: **return** $[\mathcal{G}; \mathbf{U}_1, \dots, \mathbf{U}_N]$
-

How to perform the TTMc operation at Line 4 is especially important. These TTMc’s can be performed in any order [14] using various schemes [20] that formulate TTMc in terms of multiple tensor-times-vector (TTV) operations. We now formulate TTMc in a way that specifies what to compute for each nonzero $x_{i_1, \dots, i_N} \in \mathcal{X}$ to be able to express parallelism with different task granularities. Let $\mathcal{Z} = \mathcal{X} \times_2 \mathbf{U}_2^T$ where $\mathcal{X} \in \mathbb{R}^{I_1 \times I_2 \times I_3}$, and $\mathbf{U}_2 \in \mathbb{R}^{I_2 \times J_2}$. By considering (1) for \mathcal{Z} , and performing the summation over nonzeros we obtain:

$$z_{i,t,k} = \sum_{x_{i,j,k} \in \mathcal{X}} x_{i,j,k} \mathbf{U}_2(j,t). \quad (2)$$

We can vectorize this as

$$\mathcal{Z}(i, :, k) = \sum_{x_{i,j,k} \in \mathcal{X}} x_{i,j,k} \mathbf{U}_2(j, :). \quad (3)$$

Similarly, $\mathcal{Y} = \mathcal{Z} \times_3 \mathbf{U}_3^T$ where $\mathbf{U}_3 \in \mathbb{R}^{J_3 \times J_3}$ can be written as:

$$y_{i,m,t} = \sum_{z_{i,m,k} \in \mathcal{Z}} z_{i,m,k} \mathbf{U}_3(k,t).$$

Rewriting $z_{i,m,k}$ as in (2) we get

$$y_{i,m,t} = \sum_{x_{i,j,k} \in \mathcal{Z}} x_{i,j,k} \mathbf{U}_2(j,m) \mathbf{U}_3(k,t),$$

and finally by applying (3) twice we obtain

$$\mathcal{Y}(i, :, :) = \sum_{x_{i,j,k} \in \mathcal{X}} x_{i,j,k} \mathbf{U}_2(j, :) \circ \mathbf{U}_3(k, :).$$

Specifically, for each nonzero $x_{i,j,k} \in \mathcal{X}$, we perform the outer product $\mathbf{U}_2(j, :) \circ \mathbf{U}_3(k, :)$, scale it with $x_{i,j,k}$, and then add the result to the $J_2 \times J_3$ dense matrix $\mathcal{Y}(i, :, :)$. Using the matricization of \mathcal{Y} in the first mode, this results in the following formula where a Kronecker product replaces the outer product:

$$\mathbf{Y}_{(1)}(i, :) = \sum_{x_{i,j,k} \in \mathcal{X}} x_{i,j,k} \mathbf{U}_2(j, :) \otimes \mathbf{U}_3(k, :). \quad (4)$$

For N -dimensional case, the formulation (4) generalizes to

$$\mathbf{Y}_{(n)}(i_n, :) = \sum_{x_{i_1, \dots, i_n, \dots, i_N} \in \mathcal{X}} x_{i_1, i_2, \dots, i_N} \otimes_{t \neq n} \mathbf{U}_t(i_t, :)$$

where $\otimes_{t \neq n}$ denotes the Kronecker product of $N - 1$ row vectors $\mathbf{U}_t(i_t, :)$ for $t \in \{1, \dots, N\} \setminus \{n\}$. This formulation specifies the operations performed for each nonzero element of a tensor. The resulting computation of TTMc is called nonzero-based and is given in Algorithm 2 for 3rd order tensors and $n = 1$.

Algorithm 2 Nonzero-based formulation for the mode-1 matricization of the TTMc operation $\mathcal{Y} = \mathcal{X} \times_2 \mathbf{U}_2^T \times_3 \mathbf{U}_3^T$ for 3rd order tensors

- $\mathbf{Y}_{(1)} \leftarrow 0$
for all $x_{i,j,k} \in \mathcal{X}$ **do**
 $\mathbf{Y}_{(1)}(i, :) \leftarrow \mathbf{Y}_{(1)}(i, :) + x_{i,j,k} (\mathbf{U}_2(j, :) \otimes \mathbf{U}_3(k, :))$
-

III. PARALLEL TUCKER FACTORIZATION

An efficient shared memory parallelization of the TTMc operation given in Algorithm 2 should avoid expensive lock mechanisms to resolve data dependencies. We perform a preprocessing step to organize the computations in a way that the subsequent numeric computations can be performed in parallel without any write conflicts. Following the TTMc step, computing the TRSVD of the matricized tensor $\mathbf{Y}_{(n)}$ requires special attention. Direct SVD methods that are employed to compute TRSVD in dense Tucker decomposition algorithms are not feasible for sparse Tucker decomposition due to computational and memory constraints. For this reason, we resort to iterative methods for TRSVD, which not only reduces the computational cost by exploiting the low rank of

approximation, but also renders the memory overhead due to TRSVD computation almost negligible.

For the distributed memory parallelism, we employ coarse and fine-grain task definitions. A coarse-grain task corresponds to computing a particular row $\mathbf{Y}_{(n)}(i, :)$ of the TTMc result, as well as the corresponding row $\mathbf{U}_n(i, :)$ of the factor matrix using TRSVD. In this scenario, the owner of this task possesses all the tensor nonzeros x_{i_1, \dots, i_N} where $i_n = i$. Also, each such nonzero implies data dependencies to the tasks corresponding to the rows $\mathbf{U}_1(i_1, :), \dots, \mathbf{U}_N(i_N, :)$ to be able to perform the computation of $\mathbf{Y}_{(n)}(i, :)$ using Algorithm 2. Fine-grain task definition relaxes this constraint by allowing nonzeros to be distributed freely. It associates each nonzero x_{i_1, \dots, i_N} with a task which is responsible to compute $x_{i_1, \dots, i_N} \otimes_{t \neq n} \mathbf{U}(i_t, :)$ and generate a partial result for $\mathbf{Y}_{(n)}(i_n, :)$ of size $\prod_{t \neq n} R_t$. This size is exponential in the ranks of approximation; therefore, merging the partial results can get very expensive in terms of communication, hence should be avoided. For this reason, we propose a novel method to effectively handle this communication within the TRSVD step.

A. Shared memory parallelism

1) *Parallel TTMc*: As shown in Algorithm 2, each nonzero $x_{i,j,k}$ contributes an outer product to $\mathbf{Y}_{(1)}(i, :)$, or equivalently, $\mathcal{Y}(i, :, :)$ while performing TTMc in the first mode. For shared memory parallelism, this poses a write conflict whenever two threads simultaneously process nonzeros whose first index are i . To resolve this, we make a pass over the data to compute an update list $ul_1(i)$ that holds the list of nonzeros $x_{i,j,k}$ that will contribute to $\mathcal{Y}_{(1)}(i, :)$. In the actual implementation, we only store the index t of the nonzero $x(t) = x_{i,j,k}$ to avoid duplicating the nonzero within $ul_1(i)$. In this way, we untangle the write conflicts for each row of $\mathbf{Y}_{(1)}$ and avoid using lock mechanisms. We also store the set J_1 of all indices $i \in I_1$ such that $ul_1(i) \neq \emptyset$. We repeat this computation in all dimensions, and name this step as *symbolic TTMc*, as it resolves all the index computations and dependencies once and for all outside the main loop of HOOI (shown at Lines 1-2 of Algorithm 3). This symbolic data can be reused many times for faster *numeric TTMcs* within the main loop of HOOI. Finally, symbolic TTMc of each dimension can be performed independently; hence, we perform this computation in parallel in each dimension.

After the symbolic TTMc, each row i of $\mathbf{Y}_{(1)}$ can be updated independently in parallel by using $ul_1(i)$, which composes the parallel numeric TTMc step at Lines 5–8 of Algorithm 3. In our implementation, we use OpenMP parallel loop with dynamic scheduling to distribute the tasks to threads.

2) *Parallel truncated SVD*: Following the TTMc product for mode n , HOOI requires finding the leading R_n singular vectors of the matricized tensor $\mathbf{Y}_{(n)}$ to update the matrix \mathbf{U}_n for mode n . Here, $\mathbf{Y}_{(n)}$ is of size $I_n \times (R_1 \cdots R_{n-1} R_{n+1} \cdots R_N)$. In Algorithm 3, we directly compute the matricized tensor and avoid the cost of matricization. In a recent work on parallel Tucker decomposition of dense tensors [11], leading singular vectors of $\mathbf{Y}_{(n)}$ are extracted by

Algorithm 3 Shared memory parallel HOOI

Input: \mathcal{X} : An N -mode tensor
 $\mathbf{U}_1, \dots, \mathbf{U}_N$: Initial factor matrices
 R_1, \dots, R_N : Ranks of approximation
Output: $[\mathcal{G}; \mathbf{U}_1, \dots, \mathbf{U}_N]$: Tucker approximation of \mathcal{X}

- 1: **parfor** $n = 1$ **to** N **do**
- 2: $\{ul_n, J_n\} \leftarrow \text{SymbolicTTMc}(\mathcal{X}, \{1, \dots, N\} \setminus \{n\})$
- 3: **repeat**
- 4: **for** $n = 1$ **to** N **do**
- 5: **parfor** $i \in J_n$ **do** ▶ TTMc for mode n
- 6: $\mathbf{Y}_{(n)}(i, :) \leftarrow 0$
- 7: **for all** $x_{i_1, \dots, i_N} \in ul_n(i)$ **do**
- 8: $\mathbf{Y}_{(n)}(i, :) += x_{i_1, \dots, i_N} [\otimes_{t \neq n} \mathbf{U}_t(i_t, :)]$
- 9: $\mathbf{U}_n \leftarrow \text{TRSVD}(\mathbf{Y}_{(n)}, R_n)$
- 10: $\mathcal{G} \leftarrow \mathcal{Y} \times_N \mathbf{U}_N$
- 11: **until** convergence or maximum number of iterations reached
- 12: **return** $[\mathcal{G}; \mathbf{U}_1, \dots, \mathbf{U}_N]$

computing the eigenvalues of the Gram matrix $\mathbf{Y}_{(n)} \mathbf{Y}_{(n)}^T$, where the number of rows of $\mathbf{Y}_{(n)}$, which is I_n , is typically in the order of a thousand. However, I_n can easily exceed a million for sparse tensors, rendering this method impractical for our purpose. Also, direct methods for eigenvalue and singular value problems typically compute all eigen/singular values at once, whereas in HOOI we need only R_n left leading singular value/vector pairs out of $\min(I_n, \prod_{i \neq n} R_i)$. For these reasons, we resort to using matrix-free iterative methods to compute the TRSVD of $\mathbf{Y}_{(n)}$ [18]. This way, we avoid forming the Gram matrix and compute only the required singular value/vector pairs. In the shared memory context, this TRSVD can be parallelized by using optimized BLAS2 gemv kernel for the matrix-vector (MxV) and matrix transpose-vector (MTxV) multiplications, which dominate the computational cost of the TRSVD due to the matrix being dense. As we demonstrate in the next section, this approach also enables us to reduce the communication requirements in the distributed memory setting.

After all factor matrices are updated, the core tensor is formed at Line 10 to check the convergence. Since at $n = N$, $\mathbf{Y}_{(n)}$ already holds the TTMc result $\mathcal{Y} = \mathcal{X} \times_1 \mathbf{U}_1 \times_2 \cdots \times_{N-1} \mathbf{U}_{N-1}$ in the matricized form, we multiply \mathcal{Y} with \mathbf{U}_N in mode N to obtain \mathcal{G} . Both \mathcal{Y} and \mathcal{G} are dense tensors while \mathcal{G} being significantly smaller than \mathcal{Y} ($R_1 \times \cdots \times R_N$ vs. $R_1 \times \cdots \times R_{N-1} \times I_N$). The parallel computation of dense \mathcal{G} can efficiently be performed using BLAS3, and in practice its cost should be negligible compared to the cost of sparse irregular operations carried out in computing \mathcal{Y} . We skip the details of the parallelization of Line 10 and refer the reader to a recent work by Li et al. [21].

B. Distributed memory parallelism

1) *Coarse-grain parallel HOOI*: Recall that there are two main operations for each mode n in an iteration of HOOI: a TTMc step to obtain a matricized tensor $\mathbf{Y}_{(n)}$, and an TRSVD step to obtain the matrix \mathbf{U}_n , once $\mathbf{Y}_{(n)}$ is ready. In the coarse-grain task decomposition of these computations, we define computing each row i of \mathbf{U}_n as an atomic task, and hold

the owner of this task responsible for computing the i^{th} row of $\mathbf{Y}_{(n)}$. We denote this task by t_i^n , and make the owner of t_i^n own the corresponding data elements $\mathbf{U}_n(i, :)$ and $\mathbf{Y}_{(n)}(i, :)$. For each mode n , we partition these tasks. As a result, the process p_k owns the index set I_n^k of tasks so that for each $i \in I_n^k$, t_i^n is owned by p_k .

In Algorithm 2, $\mathbf{Y}_{(1)}(i, :)$ receives a contribution $x_{i,j,k} (\mathbf{U}_2(j, :) \otimes \mathbf{U}_3(k, :))$ for each nonzero $x_{i,j,k}$. Therefore, t_i^1 needs all nonzeros in the tensor slice $\mathcal{X}(i, :, :)$, as well as the corresponding rows $\mathbf{U}_2(j, :)$ and $\mathbf{U}_3(k, :)$ to perform the Kronecker product. To compute $\mathbf{Y}_{(1)}(i, :)$, t_i^1 involves $|\mathcal{X}(i, :, :)|$ Kronecker products due to TTMc. During this computation, for each nonzero $x_{i,j,k}$, t_i^1 needs the data owned by t_j^2 and t_k^3 to perform the Kronecker product. This specifies the data to be exchanged in the communication step.

Algorithm 4 Distributed memory parallel HOOI executed at process p_k

Input: \mathcal{X}^k : Partition of \mathcal{X} owned by the process p_k
type: 'coarse-grain' or 'fine-grain'
 I_1^k, \dots, I_N^k : Set of task indices owned by p_k in each mode
 $\mathbf{U}_1, \dots, \mathbf{U}_N$: Initial factor matrices
 R_1, \dots, R_N : Ranks of approximation

Output: $[\mathcal{G}; \mathbf{U}_1, \dots, \mathbf{U}_N]$: Tucker approximation of \mathcal{X}

```

1: parfor  $n = 1$  to  $N$  do
2:    $\{ul_n, J_n\} \leftarrow \text{SymbolicTTMc}(\mathcal{X}^k, \{1, \dots, N\} \setminus \{n\})$ 
3:   if type = 'coarse-grain' then
4:      $K_n \leftarrow I_n^k$ 
5:   else
6:      $K_n \leftarrow J_n$ 
7:   repeat
8:     for  $n = 1$  to  $N$  do
9:       parfor all  $i \in K_n$  do ►TTMc for mode  $n$ 
10:         $\mathbf{Y}_{(n)}(i, :) \leftarrow 0$ 
11:        for all  $x_{i_1, \dots, i_N} \in ul_n(i)$  do
12:           $\mathbf{Y}_{(n)}(i, :) += x_{i_1, \dots, i_N} [\otimes_{t \neq n} \mathbf{U}_t(i_t, :)]$ 
13:         $\mathbf{U}_n \leftarrow \text{TRSVD}(\mathbf{Y}_{(n)}, R_n)$ 
14:        Send/receive the updated rows of  $\mathbf{U}_n$ 
15:         $\mathcal{G}^k \leftarrow \mathcal{Y} \times_N \mathbf{U}_N$ 
16:         $\mathcal{G} \leftarrow \text{AllReduce}(\mathcal{G}^k)$ 
17:   until convergence or maximum number of iterations reached
18: return  $[\mathcal{G}; \mathbf{U}_1, \dots, \mathbf{U}_N]$ 

```

Algorithm 4 gives the distributed memory parallel HOOI executed by the process p_k . Initially, we assume a partition of task indices I_n^k for each mode n , as well as the set of nonzeros \mathcal{X}^k that are needed to perform the local computations associated with these tasks. At Lines 1–6, p_k performs the symbolic TTMc with its local tensor \mathcal{X}^k . Next, at Lines 9–12 local TTMc operation $\mathbf{Y}_{(n)} \leftarrow \mathcal{X}^k \times_{-n} \mathbf{U}_n$ is performed. Note that at Line 4 we set $K_n \leftarrow I_n^k$ to make sure that the coarse-grain algorithm only computes TTMc results for the owned set of rows I_n^k . Also, p_k does not need to store the whole matrix \mathbf{U}_n ; instead, it stores the set of owned rows $\mathbf{U}_n(I_n^k, :)$, and the rows i_n that are accessed in the local TTMc computations due to $x_{i_1, \dots, i_n, \dots, i_N} \in \mathcal{X}^k$.

After the local TTMc step, we have the row-wise distributed matrix $\mathbf{Y}_{(n)}$ where p_k owns the set I_n^k of rows. For the subsequent TRSVD step, we need to perform the MxV and MTxV

multiplications $y \leftarrow \mathbf{Y}_{(n)}x$ and $x^T \leftarrow y^T \mathbf{Y}_{(n)}$. We partition the vector x blockwise. On the other hand, we partition the vector y according to I_n^k . In this way, after gathering all entries of x at all processes, the MxV operation $y \leftarrow \mathbf{Y}_{(n)}x$ can be performed locally without any communication on y entries. Also, after the TRSVD solver converges, the computed left singular vectors have the same partition as y . This way, p_k ends up having all rows $\mathbf{U}_n(I_n^k, :)$ in place, avoiding any post-communication. For $x^T \leftarrow y^T \mathbf{Y}_{(n)}$, we compute the local result $y^T \mathbf{Y}_{(n)}$, then perform an all-to-all reduction to sum up the final results in the owner processes.

In our recent work [16], we used a similar coarse-grain task definition in the context of the parallel CP-ALS algorithm, and proposed a hypergraph model for representing the computational and communication requirements of the parallel algorithm. Here, we adopt the same hypergraph model to reduce the total communication volume and to balance the computational load during the HOOI iterations. In this model, we represent tasks with vertices and their interdependence using hyperedges. The standard partitioning problem of this hypergraph corresponds to reducing the total communication volume while establishing the load balance in the TTMc step. This could also ensure load balance in the TRSVD step if the processes have almost equal number of tasks (we investigate this in our experiments). As said above, only the MTxV operation in the TRSVD step requires communication, which is regular and has a cost independent from the task distribution.

2) *Fine-grain parallel HOOI*: Coarse-grain approach has two main limitations. First, the number of tasks for a dimension n is limited by I_n . In case the tensor is very small in one of the dimensions, this poses a granularity problem by not having enough tasks for parallelism, which limits scalability. Also, coarse-grain tasks tend to be heavily interdependent with their data. As a result, there is typically little room in finding a better partition for parallelization. To address both limitations, we propose a fine-grain variant of the parallel HOOI which enables the partial computation of the rows of \mathbf{Y}_n . The fine-grain approach in Algorithm 4 differs from the coarse-grain one at Line 6, which enables computing partial results for the rows that are not owned by p_k .

Similar to the coarse-grain algorithm, we define the task t_i^n to denote the ownership of $\mathbf{U}_n(i, :)$. In the fine-grain case, the owner of t_i^n does not necessarily perform all the computations associated with $\mathbf{Y}_{(n)}(i, :)$ nor $\mathbf{U}_n(i, :)$. For each nonzero $x_{i_1, \dots, i_N} \in \mathcal{X}$, we define an associated task z_{i_1, \dots, i_N} and let the process p_k having the set of nonzeros \mathcal{X}^k also own the corresponding z -type tasks. For each mode n , the owner of z_{i_1, \dots, i_N} is responsible for performing the operation $x_{i_1, \dots, i_N} [\otimes_{t \neq n} \mathbf{U}_t(i_t, :)]$ and generating a *partial* result for $\mathbf{Y}_{(n)}(i_n, :)$. One may consider merging these partial results in a way that the owner of the task t_i^n gets the final result $\mathbf{Y}_{(n)}(i_n, :)$. This way, one can proceed with the TRSVD computation of the row-wise distributed matrix $\mathbf{Y}_{(n)}$ just as in the coarse-grain case. However, the problem in this scenario is that each partial result $\mathbf{Y}_{(n)}(i, :)$ to be communicated is of size $\prod_{i \neq n} R_i$, which is exponential in the ranks of approximation

and can easily get very large. In contrast, each message for communicating the rows of \mathbf{U}_n at Line 14 of Algorithm 4 is of size R_n .

We make use of the following observation to asymptotically reduce the communication cost due to partial results of TTMC. Performing the local TTMC with a fine-grain task distribution produces the matrix $\mathbf{Y}_{(n)}$ in the sum-distributed form $\mathbf{Y}_{(n)} = \mathbf{Y}_{(n)}^1 + \dots + \mathbf{Y}_{(n)}^N$ where $\mathbf{Y}_{(n)}^k$ is the partial TTMC result generated by the process p_k . One should avoid assembling $\mathbf{Y}_{(n)}$, otherwise a high communication overhead incurs. Fortunately, we only need to provide MxV and MTxV operations associated with the matrix $\mathbf{Y}_{(n)}$ in the subsequent TRSVD step. We can perform these multiplications without assembling $\mathbf{Y}_{(n)}$ as follows. For the MxV operation, we perform $y \leftarrow \mathbf{Y}_{(n)}^k x$ at each process p_k and generate a partial result on y . Then, we perform a point to point communication on the entries of y so that the owner of the task t_i^n sums all the partial results to obtain the final value of y_i . In this way, instead of communicating a partial result $\mathbf{Y}_{(n)}^k(i, :)$ of size $\prod_{i \neq n} R_i$, we communicate a single vector entry y_i for each i requiring communication at each iteration of the TRSVD solver. The number of TRSVD iterations is typically in the order of R_n or less, so it makes this communication cost conformal with the cost at Line 14 of Algorithm 4. We can easily perform the MTxV operation by computing $x^T \leftarrow y^T \mathbf{Y}_{(n)}^k$ at each process p_k , and then by performing an all-to-all communication on x^T just as in the coarse-grain algorithm.

We model the tasks of the fine-grain algorithm and their dependencies using the same hypergraph from our previous study [16], where we model tasks with vertices and the dependencies among tasks with hyperedges. With this model, the communication cost at Lines 13–14 of Algorithm 4 is equal to the cutsize of a partition of the corresponding hypergraph and can be effectively reduced by existing hypergraph partitioning tools. We refer the reader to [16] for the detailed analysis. We note also that by not combining the partial results of $\mathbf{Y}_{(n)}$, we increase the total computational load of matrix-vector multiplications in the TRSVD solver, as we end up having more rows than $|I_n|$ to multiply in total. Fortunately, this increase is also equal to the cutsize of the hypergraph and is significantly reduced with a good partition. Therefore, minimizing the cutsize is beneficial for reducing both the communication cost of the parallel HOOI and the redundant computation in its TRSVD step. Finally, as in the coarse-grain algorithm, the load balance in the local MxV and MTxV operations can be achieved if the MPI-ranks have equal number of rows in $\mathbf{Y}_{(n)}$. This is one of the complex partitioning problems where the total computational load can only be determined after a partition [22], [23]. We do not explicitly address this problem and hope that assigning equal amount of n -mode indices will lead to load balance.

IV. RELATED WORK

We give a brief overview of the recent progress on efficient tensor decomposition (CP and Tucker) algorithms. These can

TABLE I: Tensors used in the experiments

Tensor	I_1	I_2	I_3	I_4	#nonzeros
Netflix	480K	17K	2K	-	100M
NELL	3.2M	301	638K	-	78M
Delicious	1.4K	532K	17M	2.4M	140M
Flickr	731	319K	28M	1.6M	112M

be categorized into four classes: (i) toolboxes for Matlab and similar environments [24], [25], [26], [20], [27]; (ii) implementations for shared memory systems [28], [29], [21], [30]; (iii) implementations based on MapReduce paradigm [12], [31]; (iv) implementations for distributed memory systems [11], [32], [16], [33]. The implementations in the first group are very useful tools that enable fast prototyping. Those in the second group and similar work are helpful when data fits into the memory of a single machine, which is nowadays large enough to accommodate tensors from many applications. Those in the third and fourth groups enable computations on tensors that do not fit into the memory of a single machine. The ones in the third group are not designed for high performance, as MapReduce paradigm is meant to perform multiple passes over out-of-core data and perform global communication shuffling the input data.

To the best of our knowledge, there is no high performance distributed memory implementation of algorithms for the sparse Tucker decomposition. Among the cited references above, HaTen2 [12] is a MapReduce based HOOI implementation. Li et al. [21] investigate efficient shared memory execution of tensor times matrix products and as a future work mention how this can be used to perform intra-node TTM computations in a distributed memory setting. This work does not discuss other components of an HOOI implementation. Austin et al. [11] propose a distributed memory parallel implementation of HOOI for dense tensors. The challenges that are faced are very different from those faced in the sparse case, essentially due to all communications involving all processes, and memory accesses being regular in the dense case.

V. EXPERIMENTAL RESULTS

We conducted our experiments on an IBM Blue Gene/Q cluster, which consists of 6 racks of 1024 nodes with each node having 16 GBs of memory and a 16-core IBM PowerPC A2 processor running at 1.6 GHz. We ran our experiments up to 256 nodes (4096 cores) where we achieved the maximum scalability. Each core of PowerPC A2 can handle one arithmetic and memory operation simultaneously; therefore we assigned 32 threads per node (2 threads per core) to benefit from this. All codes we used in our benchmarks were compiled using the Clang C++ compiler (version 3.6.0) with IBM MPI wrapper using `-O3` option for compiler optimizations, and linked against IBM ESSL library for LAPACK and BLAS routines. Our code depends on PETSc and SLEPc (version 3.6.2) libraries for the distributed truncated SVD computations.

We experimented with four tensors that we formed from real world data whose properties are in Table I. Netflix tensor

has user \times movie \times time dimensions, which we formed from the data of the Netflix Prize competition [34]. In this tensor, the nonzeros correspond to the user reviews of movies, and review date extends the data to the third dimension. The values of the nonzeros are determined by the corresponding review scores given by the users. We obtained the NELL tensor from the Never Ending Language Learning (NELL) knowledge database of the “Read the Web” project [2], which consists of tuples of the form $(entity, relation, entity)$ such as (‘Chopin’, ‘plays musical instrument’, ‘piano’). The nonzeros of this tensor correspond to these entries discovered by NELL from the web, and the values are set to be the “belief” scores given by the learning algorithms used in NELL. Delicious and Flickr are the datasets for the web-crawl of Delicious.com and Flickr.com during 2006 and 2007, which is formed by Görlitz et al. [35]. These datasets consist of tuples of the form (time \times users \times resources \times tags); hence we naturally form 4-mode tensors out of these tuples.

Our parallel algorithms are independent from the partitioning method. Therefore, we use two partitioning methods to test their performance. The first partitioning method assigns the tasks uniformly at random to processes (for coarse-grain tasks we use a blocked variant), and the second one uses hypergraph partitioning tool PaToH [36]. The first method is fast, promises load balance, but it does not pay attention to the communication overhead. The second method achieves load balance, reduces communication, but is time consuming. Speedups using these two partitioning methods show the worst case behavior and the potential of the parallel algorithms, if one is willing to pay the preprocessing cost. In general, a good parallel algorithm should deliver good performance with the second partitioning method; but it should also enjoy acceptable speed up with the first partitioning method.

We used PaToH (version 3.2) with default options to partition the hypergraphs. We created all partitions offline, and ran our experiments on these partitioned tensors on the cluster. We do not report timings for partitioning hypergraphs with PaToH, which is costly. Yet in most applications, the tensors from the real-world data are built incrementally and analyzed repetitively. In this scenario, a partition for the updated tensor can be formed by refining the partition of the previous tensor. Also, one can decompose a tensor multiple times with different ranks of approximation [37]. In these cases, the time spent in partitioning can be amortized across multiple runs.

To the best of our knowledge, HaTen2 [12] is the only parallel implementation of HOOI (see Section IV). All reported parallel runtimes of HaTen2 [12] are larger than that of the sequential execution of MET algorithm [26], [20], and the sequential runtime of our method is less than that of MET. For example, on a random tensor of size $10K \times 10K \times 10K$ with 1M nonzeros, Tucker decomposition with five HOOI iterations took 87.2 seconds in MET and 11.3 seconds in our method (on a single core), including all preprocessing. This difference is expected as neither HaTen2 (which uses MapReduce) nor MET (which is a Matlab tool) are made for high performance; thus, we do not report further comparisons.

We set the ranks of approximation $R_1 = R_2 = R_3 = 10$ for the 3-mode tensors, and $R_1 = R_2 = R_3 = R_4 = 5$ for the 4-mode tensors, which is a viable choice in data analysis applications [5], [6]. We then run the parallel HOOI for 5 iterations, and report the average time spent per HOOI iteration. The symbolic TTMc is expected take much less time than the HOOI iterations. For instance, in 256-way parallel execution of Algorithm 4 using the fine-grain hypergraph partitioning for 5 iterations, symbolic TTMc took 14%, 12%, 19%, and 5% of the total execution time for Delicious, Flickr, Netflix, and NELL tensors, respectively. In general, HOOI is expected to run for more iterations; so this cost is expected to become less important. In addition, finding a good Tucker approximation of a tensor typically involves executing HOOI algorithm with various ranks [37]; symbolic TTMc can be computed once and used for all these executions.

A. Distributed memory results

In Table II, we give the strong scalability results for our distributed memory parallel HOOI algorithm. We report the average time spent per iteration in Algorithm 4. For each tensor in our dataset, we report two results for fine-grain and coarse-grain parallel algorithms (with two different partitioning methods). Those with the suffix “-hp” uses PaToH’s partitionings; “fine-rd” refers to a random partitioning, whereas and “coarse-bl” corresponds to a contiguous block partitioning of tasks. We evaluate the algorithms up to 256 compute nodes where each node executes Algorithm 4 using 32 threads. Since the amount of memory per node of Blue Gene/Q is only 16GBs, some runs were not feasible. These missing runs are shown with “-” in Table II. In two tensors, using the fine-rd partition was feasible only after 16 nodes due to higher memory requirements for storing partial results (which is proportional to the communication cost).

We first observe in Table II that in all test cases our algorithm gracefully scale up to 256 MPI ranks (or 4096 cores), except with the fine-hp partition on Netflix tensor, where we observe a slowdown at 256 nodes. On Delicious tensor, our parallel algorithm achieves 13.5x speedup using 256 nodes over the run on 8 nodes with the fine-hp partition. With the fine-rd partition, the algorithm also scales to 256 nodes, although it runs almost two times slower than fine-hp. This is expected, as fine-rd targets load balance but incurs more communication overhead. Similarly on Flickr, our parallel algorithm achieves 10.3x speedup using 256 nodes over its execution on 8 nodes with the fine-hp partition, and runs roughly twice as fast as the configuration with the fine-rd partition. Unfortunately, with Delicious, Flickr, and Netflix datasets, we were not able to get the sequential and shared memory parallel timings on a single node due to data not fitting into the memory; hence we cannot provide overall speedup results over the sequential execution. For those results, we refer the reader to a technical report [38], where we present speedups up to 742x on a different architecture with more memory. On NELL tensor, we managed to get runs on a single node. Using the fine-rd partition using 256 nodes (4096 cores),

TABLE II: Time spent per iteration (in seconds) for our distributed memory parallel HOOI using two threads per core with different partitions. Missing results are due to small amount of memory in BlueGene/Q nodes.

#nodes×#cores	Delicious				Flickr			
	fine-hp	fine-rd	coarse-hp	coarse-bl	fine-hp	fine-rd	coarse-hp	coarse-bl
1 × 16	-	-	-	-	-	-	-	-
2 × 16	-	-	-	-	-	-	-	-
4 × 16	-	-	-	-	-	-	-	-
8 × 16	164.9	-	235.3	400.5	206.2	-	287.5	308.5
16 × 16	85.2	162.0	197.5	302.4	115.6	221.8	210.5	230.1
32 × 16	47.6	96.2	155.6	206.5	64.6	124.5	166.3	190.1
64 × 16	27.2	57.8	98.9	159.6	36.8	69.9	124.1	129.0
128 × 16	18.2	34.7	80.8	96.4	22.6	42.9	87.9	102.3
256 × 16	12.2	22.1	65.1	77.1	20.0	29.2	73.8	86.3

#nodes×#cores	NELL				Netflix			
	fine-hp	fine-rd	coarse-hp	coarse-bl	fine-hp	fine-rd	coarse-hp	coarse-bl
1 × 16	222.1	222.1	240.1	240.1	-	-	-	-
2 × 16	151.6	137.6	198.5	164.4	-	-	-	-
4 × 16	87.7	75.9	180.6	131.4	33.7	39.2	46.0	42.8
8 × 16	67.8	46.9	172.5	109.7	18.6	26.1	30.6	33.4
16 × 16	54.9	28.3	112.4	94.1	10.3	18.3	32.2	27.8
32 × 16	43.9	17.2	73.8	68.2	5.7	13.9	26.2	26.7
64 × 16	35.4	11.9	67.1	54.5	3.9	10.9	26.2	21.7
128 × 16	26.7	8.4	50.3	48.5	2.9	8.7	19.8	18.7
256 × 16	14.8	7.7	48.1	44.9	3.8	8.3	14.7	16.1

we obtained 280x speedup over the sequential execution. This translates into 29x speedup over the execution on a single node. Yet, unlike other three tensors, on this data the fine-hp partition lead to slower execution than the fine-rd partition. We analyzed the underlying reason for this result on 256 MPI ranks and saw that the *maximum* communication volume per process for with the fine-hp partition in the dominant dimension was 543K in contrast to 366K in the fine-rd partition. Here, this entailed a large overhead that could not be compensated by the reduction in the total communication volume (20M vs 94M).

In Table III, we give the computation and communication requirements of one HOOI iteration on the Flickr tensor with all partitionings for 256 MPI ranks (4096 cores). In this table, \mathcal{W}_{TTMc} and \mathcal{W}_{TRSVD} correspond to the computational load of the TTMc and TRSVD steps of Algorithm 4 and Comm. vol. corresponds to the volume of send/receive communication incurred by different partitioning methods. We give both the average and the maximum values across all processes for all three metrics.

We observe in the \mathcal{W}_{TTMc} columns of Table III that TTMc work per MPI-rank is always well balanced with the fine-grain partitions. This is owing to the finer granularity of tasks which allows perfect balance. On the other hand, with the coarse-grain formulation, the TTMc tasks are not well balanced, as some tasks might be significantly more costly than others. Particularly in the TTMc computation of the 4th dimension, we observe some computational imbalance of 436% and 471% using the coarse-hp and coarse-block partitions.

We realize in the \mathcal{W}_{TRSVD} columns of Table III that the average TRSVD work \mathcal{W}_{TRSVD} given by the fine-hp partition is only slightly higher than that given by the coarse-grain partitions, which introduce no overhead to the TRSVD

computation. Particularly, \mathcal{W}_{TRSVD} is dominant in the third dimension, and the fine-hp partition results in the same total/average work (110K) as in the coarse-grain partitions. Using the random partition (fine-rd), however, the average \mathcal{W}_{TRSVD} is drastically increased to 435K in the same dimension. Moreover, even though none of the partitioning methods explicitly try to establish load balance for \mathcal{W}_{TRSVD} , we observe that the obtained load balance is generally acceptable. In the computationally dominant third mode, the fine-hp partition leads to 100% load imbalance, whereas the fine-rd, coarse-hp, and coarse-block partitions lead to 25%, 79%, and 18%.

The last two columns of Table III show the maximum and the average communication volume per process. This involves the send and receive volumes at Lines 13 and 14 of Algorithm 4. Using the fine-hp and fine-rd partitions, the average communication volumes are 11K and 1735K, respectively. Recall that the average communication volume is proportional to the cutsize of the corresponding hypergraph partition, and the cutsize equals to the total redundancy in MxV and MTxV operations. That is why we observe higher \mathcal{W}_{TRSVD} value using the fine-rd partition. The maximum communication volume per process also decreases to 166K with fine-hp partition, in comparison to 1744K using fine-rd partition. Our final observation is that fine-hp partitions are more effective in reducing the communication volume than the coarse-hp partitions.

In Table IV, we provide the relative timings of TTMc, TRSVD, and the computation of the core tensor within an iteration of HOOI using the 256-way fine-hp partition. The TRSVD timings include the time spent in the communication of the vector entries in the MxV and MTxV operations, as the communication takes place within the PETSc calls. We see in Table II that on Netflix tensor with the fine-hp partition,

TABLE III: Statistics for the computation and communication requirements with different partitionings of Flickr in one HOOI iteration for 4096-way parallel run with 256 MPI ranks.

Mode	W_{TTMc}		W_{TRSVD}		Comm. vol.	
	Max	Avg	Max	Avg	Max	Avg
<i>fine-hp</i>						
1	441K	441K	590	507	2218	2029
2	441K	441K	8778	5656	24K	17K
3	441K	441K	221K	110K	166K	11K
4	441K	441K	32K	19K	77K	53K
<i>fine-rd</i>						
1	443K	441K	668	648	5884	2597
2	443K	441K	98K	96K	409K	385K
3	443K	441K	545K	435K	1744K	1735K
4	443K	441K	110K	100K	432K	413K
<i>coarse-hp</i>						
1	718K	441K	22	3	4910	1213
2	810K	441K	2700	248	118K	66K
3	798K	441K	197K	110K	3187K	810K
4	2368K	441K	13K	6250	170K	102K
<i>coarse-block</i>						
1	958K	441K	252	3	18K	907
2	756K	441K	5401	248	126K	80K
3	441K	441K	130K	110K	3324K	1250K
4	2518K	441K	60K	6250	296K	138K

TABLE IV: Relative timings of TTMc, TRSVD, and core tensor computation steps within HOOI using 256-way fine-hp partition (in percentage)

Step	Delicious	Flickr	NELL	Netflix
TTMc	75.6	64.6	71.2	27.7
TRSVD+comm	19.2	32.6	24.8	71.6
core+comm	5.2	2.8	4.0	0.7

we lose scalability at 256 nodes. Table IV shows that for this instance TRSVD step begins to dominate the timings, and the communication cost starts to prevent further scalability. Note that in this case, the increase in the communication cost and imbalance also affects the computational cost of the TRSVD step. This is because of the fact that for each communicated vector entry there is an associated unit of redundant work in the MxV and $MTxV$ computations. We also realize in these results that the cost of forming the core tensor \mathcal{G} with a TTM followed by an AllReduce communication is negligible, as we expected. Finally, we inform that in all instances, TRSVD (as provided by SLEPc) converged in less than 5 iterations.

TABLE V: Time spent per iteration (in seconds) for shared memory parallel HOOI on node(s) with a 16-core processor. The number of MPI ranks used for each tensor is shown in the parentheses.

#threads	Delicious (8)	Flickr (8)	NELL (1)	Netflix (4)
1	1182.7	1055.8	2173.6	660.1
2	634.5	583.2	1146.3	330.8
4	361.1	354.5	616.4	167.6
8	227.5	241.6	354.1	87.3
16	173.2	201.0	252.7	48.7
32	164.9	206.2	222.7	33.7

B. Shared memory results

We evaluate the shared memory scalability of the distributed memory HOOI algorithm by varying the number of threads from 1 to 32, and using the minimum number of nodes possible. We needed 8, 8, 4, and 1 nodes to be able to execute the code on Delicious, Flickr, Netflix, and NELL, respectively, using the fine-hp partitions.

TTMc is a memory latency-bound operation; for each nonzero $x_{i,j,k}$, the access to $U_1(i, :)$, $U_2(j, :)$, and $U_3(k, :)$ likely results in a cache miss, due to the irregular pattern of nonzeros. Multi-threading is an effective way of hiding this latency; therefore it offers a great opportunity of acceleration through parallelism. However, the MxV and $MTxV$ operations in the TRSVD step are memory bandwidth-bound due to the matrices being dense. Once the memory bandwidth is saturated, one may not expect a notable speedup with multi-threading (except in a NUMA architecture where each socket has an independent memory bandwidth; yet in this case the parallelism within a socket has the same issue). The TTMc operation count is proportional to the number of nonzeros, whereas the TRSVD cost is proportional to the number of rows of the matrix (or equivalently, the size of a dimension of the tensor).

As seen in Table V, we manage to improve the runtime using 32 threads for all tensors except Flickr. Using 32 threads, the speedups we obtain for Delicious and Flickr tensors are 7.2x and 5.1x, whereas on NELL and Netflix we get 9.8x and 20x, respectively. Delicious and Flickr tensors have very large third dimension of size 17M and 28M, whereas the largest dimensions of NELL and Netflix are of size 3.2M and 480K. Therefore, NELL and particularly Netflix have more latency-bound computations and provide more room for speedup, which explains the better speedup results in comparison to Delicious and Flickr tensors. Another interesting point is that on the Netflix tensor, using 16 threads we achieve 13.8x speedup over the single threaded execution. Increasing to 32 threads results in a superlinear speedup of 20x on 16 cores. We believe that this is mostly due to each core being able to execute two threads (one for memory and one for compute operations) simultaneously, which is particularly advantageous for latency-bound sparse irregular operations.

VI. CONCLUSION

We discussed an efficient parallelization of the alternating least squares-based Tucker decomposition algorithm (HOOI, also called Tucker-ALS) for sparse tensors in shared and distributed memory systems. We introduced a nonzero-based TTMc formulation, and proposed a shared-memory parallel HOOI with a preceding symbolic computation step that uses this formulation. We proposed a coarse and a fine-grain parallel algorithm with their corresponding task definitions, and investigated the issues of load balance and communication cost reduction on different components of the the parallel algorithms. Gathering all these together, we achieved scalability up to 4096 cores using 256 MPI ranks on real world tensors with

an efficient hybrid OpenMP-MPI implementation within our high performance parallel sparse tensor library, HyperTensor.

We finally note that the TTMc operation is used in other algorithms [39] for Tucker decomposition; therefore, proposed methods of parallelism can be used by those algorithms.

ACKNOWLEDGMENT

This work was performed using HPC resources from GENCI-[TGCC/CINES/IDRIS] (Grant 2016 - i2016067501).

REFERENCES

- [1] T. G. Kolda and B. Bader, "The TOPHITS model for higher-order web link analysis," in *Proceedings of Link Analysis, Counterterrorism and Security*, 2006.
- [2] A. Carlson, J. Betteridge, B. Kisiel, B. Settles, E. R. H. Jr., and T. M. Mitchell, "Toward an architecture for never-ending language learning," in *AAAI*, vol. 5, 2010, p. 3.
- [3] K. Bollacker, C. Evans, P. Paritosh, T. Sturge, and J. Taylor, "Freebase: A collaboratively created graph database for structuring human knowledge," in *Proceedings of the 2008 ACM SIGMOD International Conference on Management of Data*. New York, NY, USA: ACM, 2008, pp. 1247–1250.
- [4] S. Rendle, B. M. Leandro, A. Nanopoulos, and L. Schmidt-Thieme, "Learning optimal ranking with tensor factorization for tag recommendation," in *Proceedings of the 15th ACM SIGKDD International Conference on Knowledge Discovery and Data Mining*, ser. KDD '09. New York, NY, USA: ACM, 2009, pp. 727–736.
- [5] P. Symeonidis, A. Nanopoulos, and Y. Manolopoulos, "Tag recommendations based on tensor dimensionality reduction," in *Proceedings of the 2008 ACM Conference on Recommender Systems*. New York, NY, USA: ACM, 2008, pp. 43–50.
- [6] Y. Xu, L. Zhang, and W. Liu, "Cubic analysis of social bookmarking for personalized recommendation," in *Frontiers of WWW Research and Development-APWeb 2006*. Springer, 2006, pp. 733–738.
- [7] C. J. Appellof and E. R. Davidson, "Strategies for analyzing data from video fluorometric monitoring of liquid chromatographic effluents," *Analytical Chemistry*, vol. 53, no. 13, pp. 2053–2056, 1981.
- [8] L. D. Lathauwer and B. D. Moor, "From matrix to tensor: Multilinear algebra and signal processing," in *Institute of Mathematics and Its Applications Conference Series*, vol. 67, 1998, pp. 1–16.
- [9] M. A. O. Vasilescu and D. Terzopoulos, "Multilinear analysis of image ensembles: TensorFaces," in *Computer Vision—ECCV 2002*. Springer, 2002, pp. 447–460.
- [10] K. Maruhashi, F. Guo, and C. Faloutsos, "MultiAspectForensics: Pattern mining on large-scale heterogeneous networks with tensor analysis," in *International Conference on Advances in Social Networks Analysis and Mining (ASONAM)*, July 2011, pp. 203–210.
- [11] W. Austin, G. Ballard, and T. G. Kolda, "Parallel tensor compression for large-scale scientific data," arXiv, Tech. Rep., 2015.
- [12] I. Jeon, E. E. Papalexakis, U. Kang, and C. Faloutsos, "Haten2: Billion-scale tensor decompositions," in *IEEE 31st International Conference on Data Engineering (ICDE)*, 2015, pp. 1047–1058.
- [13] P. Comon, "Tensors: A brief introduction," *IEEE Signal Processing Magazine*, vol. 31, no. 3, pp. 44–53, May 2014.
- [14] T. G. Kolda and B. Bader, "Tensor decompositions and applications," *SIAM Review*, vol. 51, no. 3, pp. 455–500, 2009.
- [15] L. D. Lathauwer, B. D. Moor, and J. Vandewalle, "On the best rank-1 and rank- (R_1, R_2, \dots, R_N) approximation of higher-order tensors," *SIAM Journal on Matrix Analysis and Applications*, vol. 21, no. 4, pp. 1324–1342, 2000.
- [16] O. Kaya and B. Uçar, "Scalable sparse tensor decompositions in distributed memory systems," in *Proceedings of the International Conference for High Performance Computing, Networking, Storage and Analysis*. New York, NY, USA: ACM, 2015, pp. 77:1–77:11.
- [17] S. Balay, S. Abhyankar, M. F. Adams, J. Brown, P. Brune, K. Buschelman, L. Dalcin, V. Eijkhout, W. D. Gropp, D. Kaushik, M. G. Knepley, L. C. McInnes, K. Rupp, B. F. Smith, S. Zampini, and H. Zhang, "PETSc web page," <http://www.mcs.anl.gov/petsc>, 2015.
- [18] J. E. Roman, C. Campos, E. Romero, and A. Tomas, "SLEPc users manual," D. Sistemes Informàtics i Computació, Universitat Politècnica de València, Tech. Rep. DSIC-II/24/02 - Revision 3.6, 2015.
- [19] L. D. Lathauwer, B. D. Moor, and J. Vandewalle, "A multilinear singular value decomposition," *SIAM Journal on Matrix Analysis and Applications*, vol. 21, no. 4, pp. 1253–1278, 2000.
- [20] T. G. Kolda and J. Sun, "Scalable tensor decompositions for multi-aspect data mining," in *ICDM 2008: Proceedings of the 8th IEEE International Conference on Data Mining*, Pisa, Italy, 2008, pp. 363–372.
- [21] J. Li, C. Battaglino, I. Perros, J. Sun, and R. Vuduc, "An input-adaptive and in-place approach to dense tensor-times-matrix multiply," in *Proceedings of the International Conference for High Performance Computing, Networking, Storage and Analysis*. Austin, Texas: ACM, New York, NY, USA, 2015, pp. 76:1–76:12.
- [22] K. Kaya, F. H. Rouet, and B. Uçar, "On partitioning problems with complex objectives," in *Euro-Par 2011: Parallel Processing Workshops*. Springer Berlin / Heidelberg, 2012, vol. 7155, pp. 334–344.
- [23] A. Pinar and B. Hendrickson, "Partitioning for complex objectives," in *Proceedings of the 15th International Parallel & Distributed Processing Symposium (CDROM)*. Washington, DC, USA: IEEE Computer Society, 2001, p. 121.
- [24] C. A. Andersson and R. Bro, "The N-way toolbox for MATLAB," *Chemometrics and Intelligent Laboratory Systems*, vol. 52, no. 1, pp. 1–4, 2000.
- [25] B. W. Bader and T. G. Kolda, "Efficient MATLAB computations with sparse and factored tensors," *SIAM Journal on Scientific Computing*, vol. 30, no. 1, pp. 205–231, December 2007.
- [26] B. W. Bader, T. G. Kolda *et al.*, "Matlab tensor toolbox version 2.6," Available online, February 2015.
- [27] E. E. Papalexakis, C. Faloutsos, and N. D. Sidiropoulos, "ParCube: Sparse parallelizable CANDECOP-PARAFAC tensor decomposition," *ACM Transactions on Knowledge Discovery from Data*, vol. 10, no. 1, pp. 3:1–3:25, 2015.
- [28] M. Baskaran, B. Meister, N. Vasilache, and R. Lethin, "Efficient and scalable computations with sparse tensors," in *IEEE Conference on High Performance Extreme Computing (HPEC)*, Sept 2012, pp. 1–6.
- [29] M. M. Baskaran, B. Meister, and R. Lethin, "Low-overhead load-balanced scheduling for sparse tensor computations," in *IEEE Conference on High Performance Extreme Computing (HPEC)*. Waltham, MA, USA: IEEE, Sep. 2014, pp. 1–6.
- [30] S. Smith, N. Ravindran, N. D. Sidiropoulos, and G. Karypis, "SPLATT: Efficient and parallel sparse tensor-matrix multiplication," in *29th IEEE International Parallel & Distributed Processing Symposium*. Hyderabad, India: IEEE Computer Society, May 2015, pp. 61–70.
- [31] U. Kang, E. Papalexakis, A. Harpale, and C. Faloutsos, "GigaTensor: Scaling tensor analysis up by 100 times - Algorithms and discoveries," in *Proceedings of the 18th ACM SIGKDD International Conference on Knowledge Discovery and Data Mining*. New York, NY, USA: ACM, 2012, pp. 316–324.
- [32] J. H. Choi and S. V. N. Vishwanathan, "DFacTo: Distributed factorization of tensors," in *27th Advances in Neural Information Processing Systems*, Montreal, Quebec, Canada, 2014, pp. 1296–1304.
- [33] S. Smith and G. Karypis, "DMS: Distributed sparse tensor factorization with alternating least squares," Department of Computer Science and Engineering, University of Minnesota, Tech. Rep. 15-007, May 2015.
- [34] J. Bennett and S. Lanning, "The netflix prize," in *Proceedings of KDD cup and workshop*, vol. 2007, 2007, p. 35.
- [35] O. Görnitz, S. Sizov, and S. Staab, "PINTS: Peer-to-peer infrastructure for tagging systems," in *Proceedings of the 7th International Conference on Peer-to-Peer Systems*. Berkeley, CA, USA: USENIX Association, 2008, p. 19.
- [36] Ü. V. Çatalyürek and C. Aykanat, *PaToH: A Multilevel Hypergraph Partitioning Tool, Version 3.0*, Bilkent University, Department of Computer Engineering, Ankara, 06533 Turkey. PaToH is available at <http://bmi.osu.edu/~umit/software.htm>, 1999.
- [37] H. A. L. Kiers and A. der Kinderen, "A fast method for choosing the numbers of components in Tucker3 analysis," *British Journal of Mathematical and Statistical Psychology*, vol. 56, pp. 119–125, 2003.
- [38] O. Kaya and B. Uçar, "High-performance parallel algorithms for the Tucker decomposition of higher order sparse tensors," Inria, Grenoble – Rhône-Alpes, Tech. Rep. RR-8801, Oct 2015.
- [39] L. Eldén and B. Savas, "A Newton–Grassmann method for computing the best multilinear rank- (r_1, r_2, r_3) approximation of a tensor," *SIAM Journal on Matrix Analysis and Applications*, vol. 31, no. 2, pp. 248–271, 2009.